



Surface spectators and their role in relationships between activity and selectivity of the oxygen reduction reaction in acid environments

Eduardo G. Ciapina^{a,b,c}, Pietro P. Lopes^a, Ram Subbaraman^a, Edson A. Ticianelli^c, Vojislav Stamenkovic^a, Dusan Strmcnik^{a,*}, Nenad M. Markovic^a

^a Materials Science Division, Argonne National Laboratory, Argonne, IL, USA

^b Faculdade de Engenharia, UNESP—Univ. Estadual Paulista, Guaratinguetá, SP, Brazil

^c Instituto de Química de São Carlos, Universidade de São Paulo, São Carlos, SP, Brazil

ARTICLE INFO

Article history:

Received 7 July 2015

Received in revised form 20 July 2015

Accepted 22 July 2015

Available online 29 July 2015

Keywords:

Oxygen reduction reaction

Catalyst selectivity

Electrocatalysis

Electrochemical interfaces

Electronic effects

Ensemble effects

ABSTRACT

We use the rotating ring disk (RRDE) method to study activity–selectivity relationships for the oxygen reduction reaction (ORR) on Pt(111) modified by various surface coverages of adsorbed CN_{ad} (Θ_{CNad}). The results demonstrate that small variations in Θ_{CNad} have dramatic effect on the ORR activity and peroxide production, resulting in “volcano-like” dependence with an optimal surface coverage of $\Theta_{\text{CNad}} = 0.3$ ML. These relationships can be simply explained by balancing electronic and ensemble effects of co-adsorbed CN_{ad} and adsorbed spectator species from the supporting electrolytes, without the need for intermediate adsorption energy arguments. Although this study has focused on the Pt(111)–CN_{ad}/H₂SO₄ interface, the results and insight gained here are invaluable for controlling another dimension in the properties of electrochemical interfaces.

Published by Elsevier B.V.

1. Introduction

The oxygen reduction reaction (ORR), the cathodic half-cell reaction in fuel cells [1,2], is one class of electrocatalytic reaction exhibiting strong relationships between interfacial properties and reactivity, due its multi-electron reaction nature that includes a number of elementary steps involving different reaction intermediates (e.g., O₂^{*}, H₂O₂^{*}, and OH^{*}) [3–5]. From studying the ORR on well-characterized metal single crystal surfaces it was found that the reaction kinetics varies with the crystal face differently according to the electrolyte used [6], strongly suggesting that structure sensitivity arises mainly from the geometry dependent adsorption of spectator species [7–11]. As a consequence, during the ORR metal surfaces are always covered with different kind of spectators, for which the corresponding surface coverage (Θ_s) is strongly dependent on a synergy between the substrate–adsorbate energetics, the applied electrode potential and the symmetry match between the geometry of surface atoms and adsorbates. Recently, it has been shown that a Pt(111) electrode modified by an optimal coverage of irreversibly adsorbed CN species (Θ_{CNad}) can effectively suppress adsorption of undesired tetrahedral oxyanions, while providing sufficient number of free metal sites to effectively chemisorb O₂ molecule and to break the O–O bond [12]. It was proposed that adsorption of

phosphoric and sulfuric oxyanions on Pt(111)–CN_{ad} are suppressed largely via a steric, site-blocking (ensemble) mechanism [12]. In contrast, the effect of CN_{ad} on adsorption of H_{upd} and OH_{ad} is markedly different, affecting the Pt–H_{upd} and Pt–OH_{ad} energetics via dipole–dipole CN_{ad}–H_{upd}/OH_{ad} interactions (electronic effects) [13]. Combination of these two mechanisms may serve as a basis in finding true functional links between the activity and selectivity of Pt(111)–CN_{ad} electrochemical interface in environments containing undesirable bisulfate/phosphate anions.

Given this opportunity, we decided to extend our recent rotating disk exploration of the ORR activity on the Pt(111)–CN_{ad} electrode to encompass utilization of the rotating ring disk method for monitoring CN_{ad} surface coverage dependent selective production of peroxide intermediate. Our findings address some key points in selectivity for the ORR at the same time as discuss the importance of adsorbate lateral interactions.

2. Experimental

Crystal preparation procedures and electrochemical measurements have been described in previous publications [12,14,15]. Electrode potentials are given versus the reversible hydrogen electrode (RHE), calibrated using H₂ oxidation in a separate experiment. Cyanide-modified Pt(111) electrodes were prepared by immersion of an annealed Pt(111) single crystal in 0.2 mol L^{−1} KCN solution for 30 min at open

* Corresponding author.

E-mail address: strmcnik@anl.gov (D. Strmcnik).

circuit, thus forming an irreversibly adsorbed CN adlayer. After extensive rinsing, the electrode was embedded into the rotating ring-disk electrode assembly (RRDE) and transferred into a standard three-compartment electrochemical cell containing 0.05 mol L⁻¹ H₂SO₄ (EMD) solution saturated with O₂, under potential control at 0.27 V. Electrodes with distinct θ_{CNad} were obtained by cycling the CN-modified Pt(111) electrode between 0.07 and 0.9 V in a O₂-saturated solution at 1600 rpm. Base cyclic voltammograms characteristic to a given θ_{CNad} was recorded by purging out the dissolved oxygen by argon for at least 30 min under at 0.27 V. The sweep rate for all measurements was 50 mV s⁻¹. Peroxide oxidation signal was measured at the ring held at 1.2 V. Collection efficiency found for the RRDE setup was 0.24 ± 0.05 determined from separate experiments, as described elsewhere [16]. All gases were 5 N5 quality acquired from Airgas.

3. Results and discussion

Cyclic voltammetry was used to show how the surface coverage by a “static” cyanide adlayer on Pt(111) affects the potential-dependent (“dynamic”) adsorption of H_{upd}, OH_{ad} and HSO_{4ad} in sulfuric acid solutions (Fig. 1). The voltammetric profile of Pt(111) in 0.05 M H₂SO₄ (Fig. 1a) is divided in three potential regions: (i) the H_{upd} potential region between 0.05 V and 0.35 V; (ii) adsorption of (bi)sulfate ions between 0.35 V and 0.6 V, with a distinctive sharp adsorption peak (so-called butterfly peak) related to disorder–order transition of HSO_{4ad} [17,18]; and (iii) 0.6 to 0.9 V where a small hump corresponds to OH_{ad} adsorption. For comparison, the cyclic voltammetric (CV) profile of Pt(111) in 0.1 M HClO₄ is displayed in Fig. 1a. Consistent with the previous literature [12], while there is no difference in the H_{upd} region between these two electrolytes, in 0.1 M HClO₄ a characteristic reversible peak centered at 0.8 V (also called the butterfly feature) corresponds to adsorption of OH⁻. Nevertheless, Fig. 1b–f show that in sulfuric acid solution the potential-dependent adsorption of spectator species is altered on the Pt(111)–CN_{ad} electrode. Three characteristic voltammetric features are noteworthy. First, the H_{upd} region is extended up to ca. 0.6 V, suggesting the existence of electrostatic interactions (dipole–dipole forces) between partially positively charged H_{upd} and a partially negatively charged CN_{ad}. Notice also that while between 0.05 and 0.4 V the adsorption profile (peak shape) on Pt–CN–H_{upd} is consistent with a Frumkin-like adsorption, at more positive potential the

adsorption of H_{upd} is also controlled by some attractive forces between CN_{ad} and H_{upd}. Second, the formation of the butterfly feature in region (ii) is rapidly suppressed even at $\theta_{\text{CNad}} = 0.04$ ML, confirming previous observation that an ordered adsorption of bisulfate anions requires large ensemble of Pt surface sites. A close inspection of Fig. 1 reveals that increase by CN_{ad} to 0.16 ML leads to a further decrease in θ_{HSO4ad} so that at ca. $\theta_{\text{CNad}} = 0.31$ ML the adsorption of HSO₄ is observed only above 0.6 V (a small increase in the “double layer” pseudocapacitive feature). Complete suppression of bisulfate anions appears to occur on the surface which is covered by $\theta_{\text{CNad}} = 0.36$ ML. Third, the surface coverage and the potential window of adsorption of OH_{ad} are also dependent on θ_{CNad} . Due to decrease in the surface coverage by HSO_{4ad} an initial enhanced OH adsorption is observed already at $\theta_{\text{CNad}} = 0.04$ ML (a peak at 0.9 V). Further increase in θ_{CNad} , however, is first mirrored by the concomitant increase in θ_{OHad} , that later becomes suppressed for $\theta_{\text{CNad}} > 0.31$ ML. It is reasonable to suggest that the observed relationship between θ_{CNad} and θ_{OHad} is controlled by a delicate balance between the surface coverage by CN_{ad} and bisulfate anions and thus the availability of Pt sites for OH_{ad} formation that requires a single Pt site. Unlike H_{upd}, the peak potential for OH_{ad} is shifted towards more positive potentials relative to one observed in perchloric acid solution because of the existence of lateral repulsion between partially negative charges of CN_{ad} and OH_{ad}. All of these changes observed for the “dynamic” spectators can be related to the nature of the Pt–cyanide bonding and its surface structure, as they can interact through both electrostatic forces and site ensemble selectivity. Taken together, we conclude that CN_{ad} “static” layer can affect adsorption of “dynamic” adsorbates by either modifying or eliminating surface site-ensembles and by electrostatic dipole–dipole forces.

In our previous work we used rotating disk electrode (RDE) method to study the ORR on Pt(111) modified by an optimal coverage of CN_{ad} [12]. Of concern here is to monitor how the peroxide formation depends on various surface coverages of both the “static” and “dynamic” spectators. For monitoring simultaneously the ORR and concomitant peroxide formation we employed the RRDE method. Selected polarization curves for the ORR on Pt(111)–CN_{ad} disk electrode and corresponding peroxide oxidation currents on the ring electrode are summarized in Fig. 2a and b, respectively, also including the results on Pt(111) in 0.1 M HClO₄, for comparison. Qualitatively, peroxide formation occurs below 0.5 V, e.g., in the “double layer” and H_{upd} potential regions. For our purposes

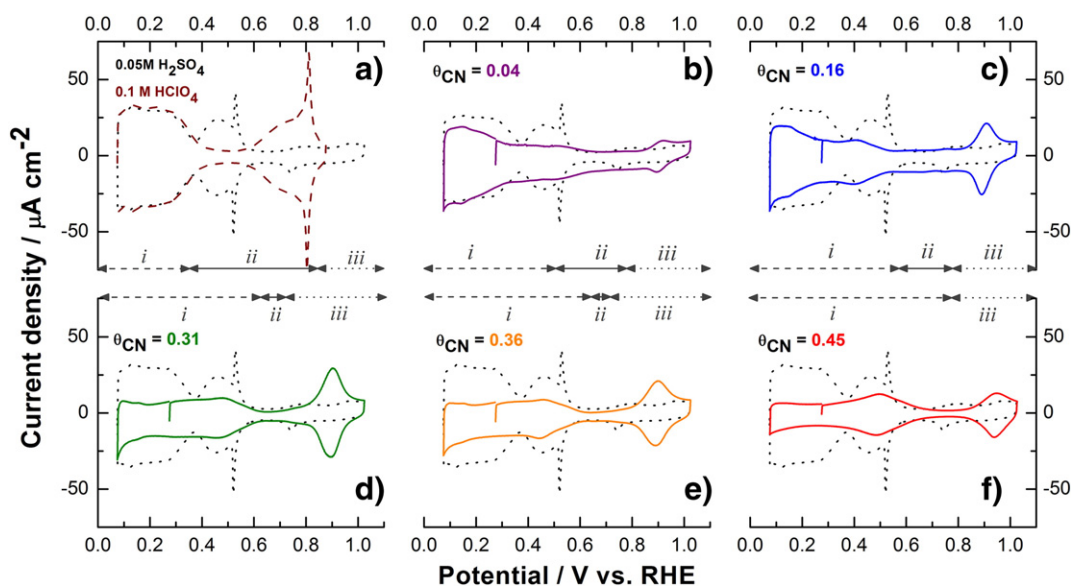


Fig. 1. Cyclic voltammograms of Pt(111)–CN_{ad} electrode in several distinct CN_{ad} coverages in 0.05 mol L⁻¹ H₂SO₄ electrolytes. a) bare Pt(111) in both H₂SO₄ and HClO₄. (b) Pt(111) covered with $\theta_{\text{CNad}} = 0.04$ ML, (c) 0.16 ML, (d) 0.31 ML, (e) 0.36 ML and (f) 0.45 ML. Potential region i (dashed), ii (solid) and iii (dotted) highlights the presence of H_{upd}, adsorbed (bi)sulfate and OH_{ad}, respectively. All experiments were conducted at 25 °C with 50 mV s⁻¹ sweep rates.

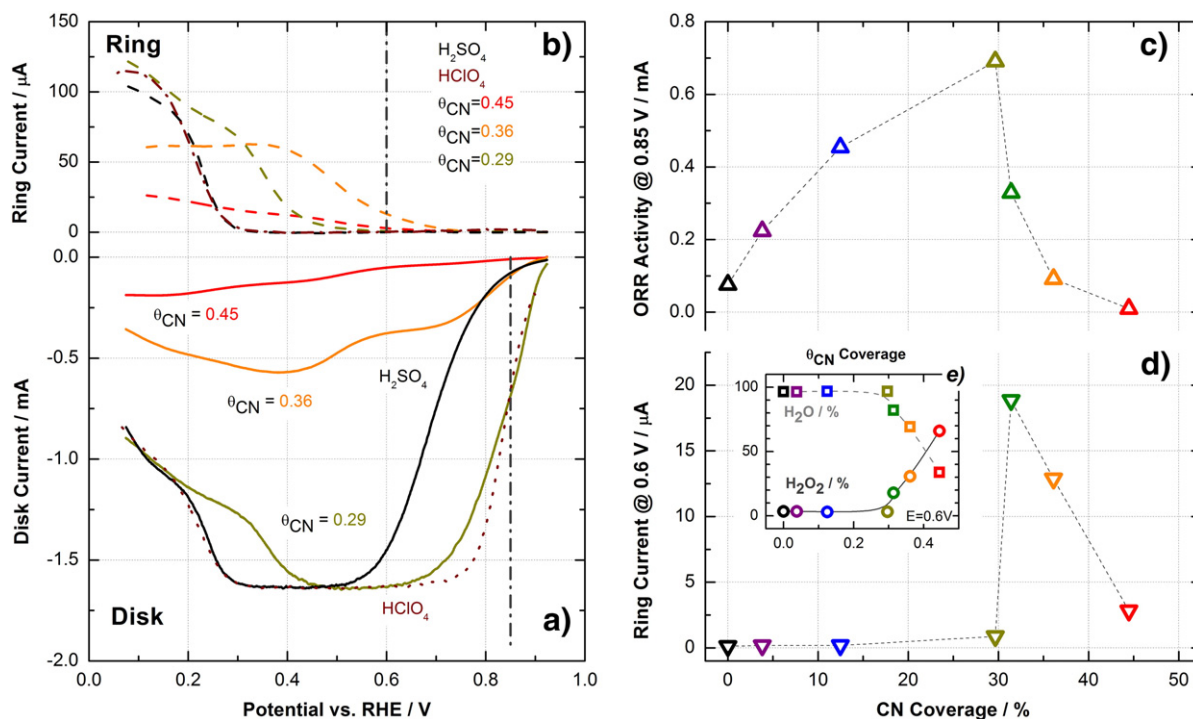


Fig. 2. RRDE results for ORR in Pt(111)–CN_{ad} electrode in several distinct CN_{ad} coverages in 0.05 mol L^{−1} H₂SO₄. The disk and ring currents are shown in a) and b), respectively. Polarization curves for Pt(111) in pure HClO₄ are included for comparison. “Volcano”-like trend with varying θ_{CNad} was measured at 0.85 V for activity (c) and peroxide production at 0.60 V (d). ORR selectivity determined at 0.60 V is shown in (e), using Eq. (1). Note that H₂O₂ is only produced below the reversible potential for $\text{O}_2 + 2\text{H}^+ + 2\text{e}^- \rightarrow \text{H}_2\text{O}_2$.

here we will first focus on the role of CN_{ad} on the reaction pathway and then we use the RRDE polarization curves recorded in Fig. 2a and b to explore the manner and extent of Pt–OH_{ad} and Pt–H_{upd} interactions may affect the ORR on Pt(111)–CN_{ad}.

As expected, activity–selectivity relationships are strongly dependent on the θ_{CNad} . A quantitative analysis of the results depicted in Figs. 1a–f, 2a and b, summarized in the form of θ_{CNad} vs. ORR activity at 0.85 V (Fig. 2c) and θ_{CNad} vs. ring currents at 0.6 V (Fig. 2d) provides insight into the role of the surface coverage of adsorbed species (θ_s) on the rate of the ORR and peroxide production. While 0.85 V was chosen because in this region the ORR is under kinetic control, 0.6 V is an optimal potential where the role of CN_{ad} can be studied without an interference with the H_{upd} potential region. Notice that by changing θ_{CNad} the surface coverage by bisulfate will affect the activity of ORR (blocking O₂ adsorption) but not the peroxide production after the ORR starts. This is because desorption of large bi-sulfate anions leave behind an ensemble of at least four Pt sites that are required for further reduction of H₂O₂* to water (see the result for the ORR on Pt(111) in 0.05 M H₂SO₄). Thus, one can anticipate that at 0.6 V it is indeed possible to explore the role of CN_{ad} on the functional links between activity and selectivity. Fig. 2e shows the fraction of H₂O₂* ($x_{\text{H}_2\text{O}_2}$) produced at 0.6 V as well as the production of H₂O (a 4e[−] process). The fraction of peroxide is calculated using the equation: [16,19]:

$$\text{H}_2\text{O}_2(\%) = \frac{2I_{\text{ring}}/N}{I_{\text{disk}} + (I_{\text{ring}}/N)} \quad (1)$$

where I_{ring} and I_{disk} are ring and disc currents at 0.6 V and N is the collection efficiency (determined as 0.24). As expected, for high CN_{ad} coverages ($\theta_{\text{CNad}} > 0.36$ ML) very small currents for ORR are observed, signaling that the Pt sites for adsorption of O₂ are highly blocked by CN_{ad}. This observation is in harmony with CVs depicted in Fig. 1e to f, and with the fact that at high θ_{CNad} on Pt(111) adopts an ordered close packed structure [20–22]. Even more striking is the effect of CN_{ad} on the selectivity, as for $\theta_{\text{CNad}} > 0.31$ ML the ORR almost entirely

goes through the 2e[−] pathway generating H₂O₂ (see Fig. 2e). As proposed above, under this experimental conditions the selectivity is predominantly governed by the lack of large Pt ensembles (at least 4 Pt atoms) needed to further reduce H₂O₂* to water. As expected, Fig. 2c and d show a θ_{CNad} -controlled “volcano” like behavior; e.g., by decreasing the θ_{CNad} the ORR first increases, reaching its maximum for $\theta_{\text{CNad}} = 0.29$ ML, and then decreases so that for $\theta_{\text{CNad}} < 0.1$ ML the activity approaches same as on bare Pt(111) in sulfuric acid solution (Fig. 2a).

Also worth noting briefly is that in certain potential range the activity–selectivity relationships are controlled by the combined effects of θ_{CNad} and θ_s of dynamic spectators. Two potential regions are of particular interest; namely, the potential window where on Pt(111)–CN_{ad} surface either OH_{ad} or H_{upd} are adsorbed on CN_{ad}-free Pt sites (see Fig. 1, regions i and iii). In contrast to adsorption of bisulfate ions, these two dynamic spectators need only one Pt site for adsorption. It is reasonable to anticipate that reactivity and selectivity will depend strongly on the intermolecular interactions between adsorbed species. For example, the onset potential for the ORR is strongly dependent on θ_{OHad} , the effect arising from the need of removal (reduction) of OH_{ad} that is controlling adsorption of O₂. Interestingly, irrespectively of θ_{CNad} the ORR below 0.8 V (region iii, Fig. 1) proceeds without peroxide formation. In contrast, for the same CN_{ad} coverages in the H_{upd} potential region the ORR is always accompanied by peroxide production. A possible origin for this difference could be due both distinct nature of H_{upd}–H_{upd} vs. OH_{ad}–OH_{ad} interactions and/or the role H_{upd} and OH_{ad} may have in the overall reaction pathway. For instance, while H_{upd} tends to form a randomly distributed disordered structure (the Frumkin-type isotherm with repulsive lateral interactions), it appears that OH_{ad} adlayer has a tendency to cluster on the Pt(111) surface, at least at lower OH_{ad} coverages. As a consequence, a small θ_{Hupd} can alter significantly the availability of Pt ensembles required for breaking the O–O bond in H₂O₂; thus acting as a third-body effect. On the other hand, if OH_{ad} has a tendency to cluster on the Pt(111) surface then there are always free sites (ensemble of four atoms) for further reduction of the peroxide intermediates. Clearly, the interactions observed between

static and dynamic spectators can help us to infer not only that certain ensemble of Pt sites is required for the $4e^-$ reduction but, in addition, provide more substantial evidence on how the switching between the “peroxide pathway” and the “water pathway” might take place.

4. Conclusion

By combining the use of a “static” spectator, (CN_{ad} , with a known surface coverage) with the common “dynamic” spectators observed in sulfuric acid solutions (H_{upd} , HSO_{4ad} and OH_{ad}) we were able to propose the functional links between activity and selectivity for the ORR. These relationships can be simply explained by balancing electronic and ensemble effects of adsorbed spectators without invoking intermediate adsorption energy arguments. Although this study has focused on the Pt(111)– CN_{ad}/H_2SO_4 interface, the results and insight gained here are valuable for controlling another dimension in the properties of electrochemical interfaces.

Acknowledgments

This work was supported by the Office of Science, Office of Basic Energy Sciences, Division of Materials Sciences, U.S. Department of Energy, under contract DE-AC02-06CH11357 (BES-DMSE). E. G. Ciapina acknowledges support from FAPESP (grant numbers 2010/02905-2 and 2013/16930-7).

References

- [1] H.A. Gasteiger, N.M. Markovic, *Chemistry. Just a dream—or future reality?* Science 324 (2009) 48–49.
- [2] M.K. Debe, *Electrocatalyst approaches and challenges for automotive fuel cells*, Nature 486 (2012) 43–51.
- [3] M.H. Shao, R.R. Adzic, *Spectroscopic identification of the reaction intermediates in oxygen reduction on gold in alkaline solutions*, J. Phys. Chem. B 109 (2005) 16563–16566.
- [4] N. Ohta, K. Nomura, I. Yagi, *Adsorption and electroreduction of oxygen on gold in acidic media: in situ spectroscopic identification of adsorbed molecular oxygen and hydrogen superoxide*, J. Phys. Chem. C 116 (2012) 14390–14400.
- [5] J.K. Nørskov, J. Rossmeisl, A. Logadottir, L. Lindqvist, J.R. Kitchin, T. Bligaard, et al., *Origin of the overpotential for oxygen reduction at a fuel-cell cathode*, J. Phys. Chem. B 108 (2004) 17886–17892.
- [6] N.M. Markovic, P.R. Jr, *Surface science studies of model fuel cell electrocatalysts*, Surf. Sci. Rep. 45 (2002) 117–229.
- [7] F.C. Nart, T. Iwasita, M. Weber, *Vibrational spectroscopy of adsorbed sulfate on Pt(111)*, Electrochim. Acta 39 (1994) 961–968.
- [8] F.C. Nart, T. Iwasita, *An FTIR study of adsorbed sulfate species on polycrystalline platinum with application of group theory to the problem of band assignment for adsorbed species*, J. Electroanal. Chem. 322 (1992) 289–300.
- [9] V.R. Stamenkovic, N.M. Markovic, P.N. Ross, *Structure-relationships in electrocatalysis: oxygen reduction and hydrogen oxidation reactions on Pt (111) and Pt (100) in solutions containing chloride ions*, J. Electroanal. Chem. 500 (2001) 44–51.
- [10] N.M. Markovic, H.A. Gasteiger, B.N. Grgur, P.N. Ross, *Oxygen reduction reaction on Pt(111): effects of bromide*, J. Electroanal. Chem. 467 (1999) 157–163.
- [11] H.A. Gasteiger, N.M. Markovic, P.N. Ross, *Bromide adsorption on Pt (111): adsorption isotherm and electrosorption valency deduced from RRD Pt (111) E measurements*, Langmuir 12 (1996) 1414–1418.
- [12] D. Strmcnik, M. Escudero-Escribano, K. Kodama, V.R. Stamenkovic, A. Cuesta, N.M. Markovic, *Enhanced electrocatalysis of the oxygen reduction reaction based on patterning of platinum surfaces with cyanide*, Nat. Chem. 2 (2010) 880–885.
- [13] M. Escudero-Escribano, G.J. Soldano, P. Quaino, M.E. Zoloff Michoff, E.P.M.M. Leiva, W. Schmickler, et al., *Cyanide-modified Pt(111): structure, stability and hydrogen adsorption*, Electrochim. Acta 82 (2012) 524–533.
- [14] D.S. Strmcnik, P. Rebec, M. Gaberscek, D. Tripkovic, V. Stamenkovic, C. Lucas, et al., *Relationship between the surface coverage of spectator species and the rate of electrocatalytic reactions*, J. Phys. Chem. C 111 (2007) 18672–18678.
- [15] B. Genorio, D. Strmcnik, R. Subbaraman, D. Tripkovic, G. Karapetrov, V.R. Stamenkovic, et al., *Selective catalysts for the hydrogen oxidation and oxygen reduction reactions by patterning of platinum with calix[4]arene molecules*, Nat. Mater. 9 (2010) 998–1003.
- [16] U.A. Paulus, T.J. Schmidt, *Oxygen reduction on a high-surface area Pt/Vulcan carbon catalyst: a thin-film rotating ring-disk electrode study*, J. Electroanal. Chem. 495 (2001) 134–145.
- [17] A.M. Funtikov, U. Stimming, R. Vogel, *Anion adsorption from sulfuric acid solutions on Pt(111) single crystal electrodes*, J. Electroanal. Chem. 428 (1997) 147–153.
- [18] N. García, V. Climent, J.M. Orts, J.M. Feliu, A. Aldaz, *Effect of pH and alkaline metal cations on the voltammetry of Pt(111) single crystal electrodes in sulfuric acid solution*, ChemPhysChem 5 (2004) 1221–1227.
- [19] J.S. Jirkovský, M. Halasa, D.J. Schiffrin, *Kinetics of electrocatalytic reduction of oxygen and hydrogen peroxide on dispersed gold nanoparticles*, Phys. Chem. Chem. Phys. 12 (2010) 8042–8052.
- [20] A. Cuesta, *At least three contiguous atoms are necessary for CO formation during methanol electrooxidation on platinum*, J. Am. Chem. Soc. 128 (2006) 13332–13333.
- [21] C. Stuhlmann, I. Villegas, M.J. Weaver, *Scanning tunneling microscopy and infrared spectroscopy as combined in situ probes of electrochemical adlayer structure. Cyanide on Pt(111)*, Chem. Phys. Lett. 219 (1994) 319–324.
- [22] C. Stuhlmann, *Characterization of an electrode adlayer by in-situ infrared spectroscopy: cyanide on Pt(111)*, Surf. Sci. 335 (1995) 221–226.